

Determination of Activation Energy For Static Re-Crystallization in Nb-Ti Low Carbon Micro Alloyed Steel

Abdulnaser Hamza Fadel
Al Zawia University, Faculty of Natural Resources

Al Zawia , Libya
Naser.fadel2369@gmail.com

Nenad Radović
University of Belgrade, Faculty of Technology and
Metallurgy, Department of Metallurgical Engineering
Belgrade, Serbia
Karnegijeva 4, 11120 Belgrade, Serbia

Abstract – Data required for calculation the static re-crystallization kinetics have been evaluated from laboratory simulations. Series of two hit isothermal tests were conducted on high temperature torsion machine. These tests were conducted on four different temperatures and using inter-pass times between 0.5 and 5s with aim to investigate the influence of thermal activation on static re-crystallization. All tests were conducted on temperatures over T_{NR} temperature, i.e. in temperature range in which all niobium is present only in solid solution. Method of evaluation of re-crystallization fraction was mechanical metallography, i.e. evaluation based on shape of each stress-strain curve. The fraction softening was calculated for all temperatures, together with avrami exponent, n_A , and activation energy for re-crystallization, Q_{SRX} . Activation energy for static re-crystallization $Q_{SRX} = 281$ KJ/mol and avrami exponent $n_A = 1$ determined in this work are in excellent agreement with previously reported data.

Index Terms: Micro-alloyed steels, Static Re-Crystallization, Fractional Softening, Activation Energy.

I. INTRODUCTION

The low carbon steels containing, niobium Nb, vanadium V, and titanium Ti in total amount of 0.15 % are usually identified as micro-alloyed steels. The micro-alloyed steels compared with carbon steels offer not only a higher yield strength, which in most cases permits savings in weight or prolonged service life of components and structures but also favorable working properties, such as improved formability and weld-ability, and resistance to hydrogen induced or stress corrosion cracking [19]. The typical structural changes occurring during intervals between hot rolling passes of austenite are static recovery, static re- crystallization and strain

induced precipitation. These structural changes play an important role in determining the final microstructure and properties of high strength low alloy steels (low carbon steels containing Nb, V and Ti in total amount of 0.15%). To obtain a desirable combination of mechanical properties, a good understanding of the underlying physical metallurgy of static restoration processes is needed, and a proper control of their occurrence is required. The micro-alloyed steels are steels in which small addition of alloying elements lead to intensive grain refinement and/or precipitation hardening due to precipitation of stable carbides, nitrides or carbonitrides [18]. Nowadays low carbon steels are alloyed with Nb and/or V and/or Ti, these elements share the common feature of precipitation of carbonitrides and/or carbides/nitrides on temperatures of hot working. They are produced as hot-rolled products, usually using controlled rolling technology. Roughing stage should be performed in temperature region in which full re-crystallization takes place, and finish rolling should be performed in temperature region in which static re-crystallization should be inhibited or suppressed. In the case of reverse finish rolling (long interpass times), the re-crystallization suppression is due to precipitation of carbonitrides, i.e. precipitates block the grain boundaries, do not allow its motion. In the case of finish short interpass times, the re-crystallization suppression is due to presence of micro-alloying elements in solid solution, i.e. soluted atoms decrease the grain boundary mobility. High strength of micro-alloyed steels is based on very fine ferritic grain, and additionally some very fine precipitation strengthening. After finishing the rolling process, microstructure consists of un-recrystallized austenite grains, with increased dislocation density and deformation bands is produced. Following the ferrite nucleation, this can occur on considerably larger number of sites, resulting in very fine grain structure. Therefore, knowledge of re-crystallization and its possible interaction with precipitation is of great importance. The main task of controlled rolling of micro-alloyed (MA) steels is to obtain a structure consisting of uniform small ferrite grains, providing good mechanical and technological properties. These demands have imposed

Received 28 February 2017; revised 15 March 2017; accepted 7 May 2017.

Available online 8 May 2017.

an extensive research, targeting mechanisms and kinetics of all processes occurring during hot rolling (i.e. re-crystallization, precipitation, in either dynamic or static conditions) [1-6]. One direction of the research was focused on static re-crystallization (SRX) behavior. The description of SRX kinetics and influences of processing parameters are most usually, in a Johnson–Mehl–Avrami–Kolmogorov manner [7, 8]. The values of activation energy for static re-crystallization, Q_{SRX} for most of micro-alloyed steels, in high temperature range have been reported to be between 240 and 450kJ/mol, mainly due to differences in chemical composition [1-6]. Medina and Quispe [3] reported an improved model that take in account the influence of chemical composition on Q_{SRX} , in the temperature range above SRCT, i.e. in temperature range in which alloying elements are in solid solution. These studies were carried out on laboratory scale, at constant temperature (isothermally). On the other hand, re-crystallization behavior during continuous cooling (conditions close to industrial practice) was investigated mainly with the aim to determine the no recrystallization temperature, T_{nr} , in the manner introduced by Boratto et al. [1]. The aim of this work was to determine the activation energy for static recrystallization in the temperature region above T_{nr} temperature, i.e. temperatures at which micro alloyed elements are in solid solution.

II. EXPERIMENTAL

The steel used for this investigation was low carbon Nb/Ti micro alloyed steel. Chemical composition of tested steel is given in table 1. The steel was produced and continuously casted on vertical continuous caster in steel works, as casted slabs were hot-rolled in Hot Strip Mill. Specimens were taken from pre-rolled strip (thickness 30mm) in direction parallel to rolling direction and before machining the specimens, the steel was annealed at 1050 °C for three hours in protective

Table1. Chemical Composition of Steel Investigated

element	C	Mn	Si	P	S
Wt %	0.074	1.15	0.21	0.024	0.013
element	Al	Mo	Nb	Ti	N
Wt %	0.068	0.023	0.035	0.016	0.009

atmosphere, with aim to remove texture and for homogenization. The specimen dimensions used in the high temperature torsion testing are as shown in figure 1 with diameter and gauge length of 6 and 50 mm respectively as shown in figure 1. The scheme and the hot temperature torsion machine is shown in figure 2. The main purpose of high temperature torsion machine is the simulation of hot deformation processes (both single-pass and multi-pass) on high temperatures. The main advantage of this machine in comparison to compression or tensile testing is the ease in obtaining strain that is present in hot rolling practice. Achievable strains in compression or tensile testing is limited to small extent due to appearance of bucking and necking respectively.

The machine is equipped with a low-inertia motor with additional gear, enabling rotation from one to 1500 turns in one minute. The Motor is controlled by hronometer, which controls the time for motor rotation. Induction heater, cooled with water, is connected with optical pyrometer and thermo-regulator. Both of latter regulate the power of the heater. For temperature measurement optical pyrometer measures the emissivity of specimen surface. Reliable measurements are within temperature range 750 – 1300 °C. To provide good surface quality, specimens are treated in protective atmosphere, because emissivity can be wrong if oxidation occurs.

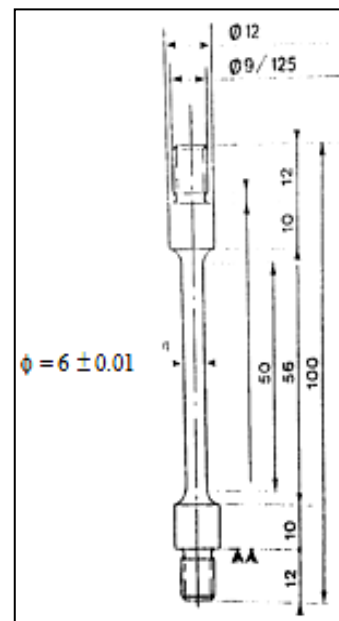


Fig.1. Specimen for Torsion Testing.

For measuring the torque, a dynamometer with range of 0 – 7 Nm is used. Measured values are recorded both on photo-paper and in data acquisition system provides complete communication with torsion tester via PC computer. Resolution of automatic measurements system is 60 measurements for one turn, i.e. on each 6°. Measured values are automatically recorded on PC.

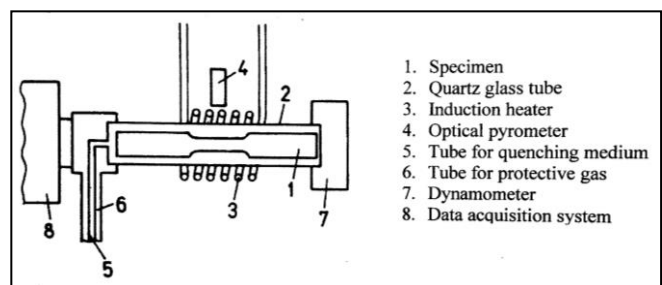


Figure.2. Scheme of Hot Temperature Torsion Machine.

To obtain data necessary for determination of static re-crystallization kinetics a set of two-hit isothermal at different temperatures was performed. In previous work [6], T_{nr} of 937 °C was obtained, so that temperatures

range in which Nb is still in solid solution is above this temperature. The two-hit isothermal test experimental details is given in table 2 and scheme of isothermal testing is shown in figure 3.

Table2. Two-Hit Isothermal Test Experimental Details

Temperature, °C	965,1000,1050,1100
Strain per pass	0.35
Strain rate, s ⁻¹	1.5
Interpass, s	0.5,0.75,1.0,1.5,2.0,2.5,3.0,3.5,4.0,4.5,5.0

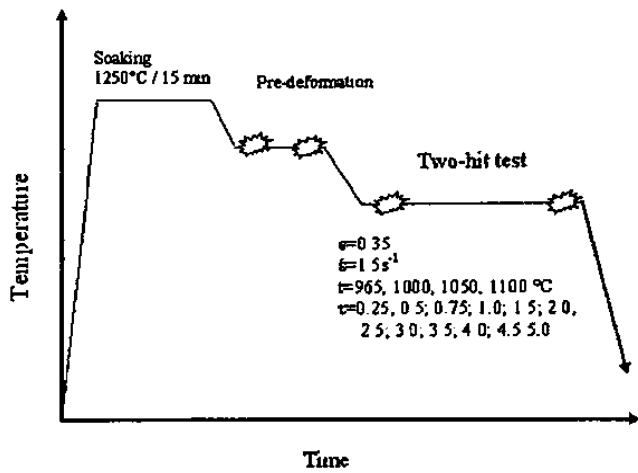
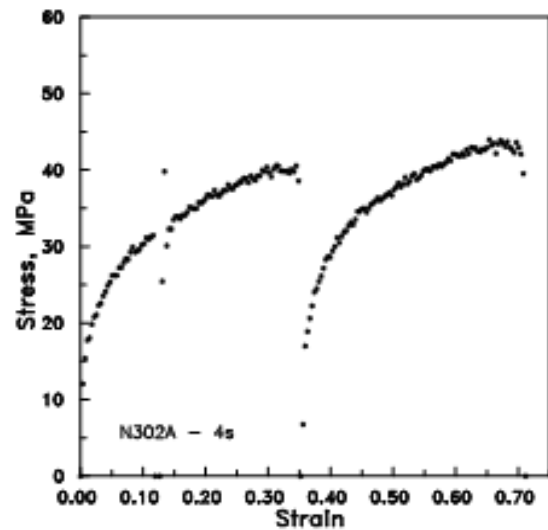


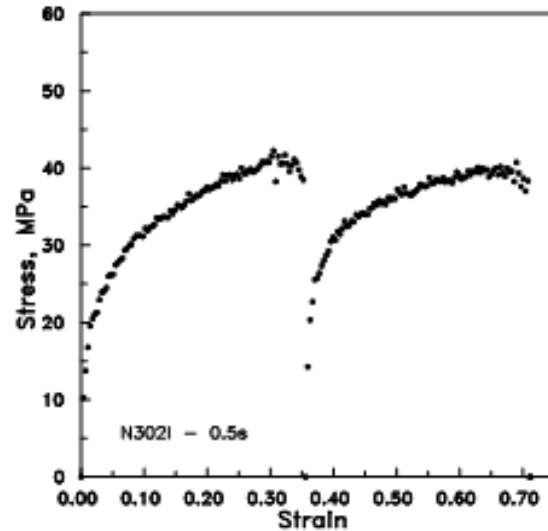
Figure.3. Scheme of Isothermal Two-Hit Testing.

III. RESULTS

Flow curves. The representative sets of two hit flow curves are shown in figures 4 (a) and (b). In the first pass, there is continuous increase in flow stress. The flow curve is characterized by both low yield strength and a high strain-hardening rate. This kind of behavior was recorded in all tests. In the second pass, depending on interpass time, flow curve can have different shapes. In the case of longer interpass times, figure 4a, or higher temperatures, shape of the curve is similar to flow curve in the first pass, i.e. low yield point and higher strain rate. On the other hand, in some cases, as shown in Fig. 4 (b), the shape of flow curve in second pass exhibits much higher yield point, and subsequent lower strain hardening rate.



(a)



(b)

Figure 4. Stress-Strain curves obtained in two hit torsion tests

($\epsilon_1 = 0.35$, $\dot{\epsilon} = 1.5 \text{ s}^{-1}$, $T = 1000 \text{ °C}$).

(a) Longer interpass time. (b) Shorter interpass time.

Fractional Softening-Interpass Time Curves. The isothermal interpass softening is calculated for each test, in the manner proposed by [2,4], using 0.1% offset method (there are several methods for calculation of fractional softening on the basis of the changes of flow curves). Times of 50% of softening were estimated and given in table 3.

Table3. Time for 50% Fractional Softening on Different Temperatures.

Temperature, °C	t _{0.5, s}
1100	0.1
1050	0.3
1000	0.75
965	1.75

Avrami kinetics. As mentioned before, the description of SRX kinetics and influences of processing parameters are mostly, in a Johnson-Mehl-Avrami-Kolmogorov manner or more often Avrami equation i.e.

$$X_{SRX} = 1 - \exp(-k \cdot t^{n_{SRX}}) \tag{1}$$

After double ln of equation 1:

$$\ln \ln \frac{1}{1-f} = \ln k + n_{SRX} \cdot \ln t \tag{2}$$

However equation (1) can be rewritten as:

$$X_{SRX} = 1 - \exp\left[-0.693\left(\frac{t}{t_{0.5}}\right)^{n_{SRX}}\right]$$

$$t_{0.5} = A_{SRX} \exp\left(\frac{Q_{SRX}}{RT}\right) \tag{3}$$

Where:

X-recrystallized fraction, n-Avrami exponent, t-time, t_{0.5}-time for 50% recrystallization, calculated using following equation [2], A_{SRX}-constant, T-absolute temperature, R-universal gas constant and Q_{SRX}-activation energy for static recrystallization.

Avrami exponent or constant (n_{SRX}) was calculated by rearranging equation (2) and is derived as the slope from equation (2) as shown in figure 5.

Figure 5 is shows a typical fractional softening vs. time dependence, obtained at 965 °C and from this diagram, slope is indicating the Avrami exponent. In all cases lines are straight on all temperatures, showing single slope and obtained results are given in table 4.

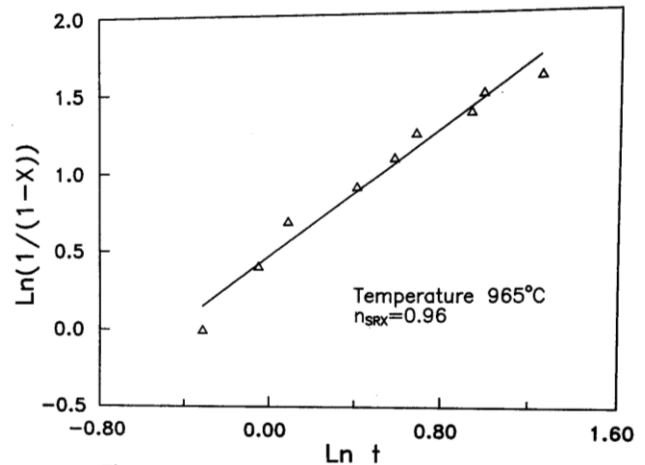


Fig.5. Fractional Softening vs. Time Dependence at 965°C.

Table 4. Avrami Exponent Estimated on Different Temperatures.

Temperature, °C	n _{SRX}
1100	1.03
1050	1.01
1000	1.02
965	0.96
Average value	1.00 ± 0.03

The activation energy for static recrystallization was calculated after rearranging equation (3).

$$\ln t_{0.5} = \ln A_{SRX} + \frac{Q_{SRX}}{R} \cdot \frac{1}{T} \tag{4}$$

Ln t vs. 1/T dependence is shown in figure 6, based on data from table 3. The slope on this figure determines the activation energy Q_{SRX} and the intercept is equal to ln A_{SRX}. The value of activation energy for static recrystallization for low carbon Nb/Ti micro-alloyed steel obtained in this work is equal to 281 kJ/mol and A_{SRX} is equal to 2.21 × 10⁻¹².

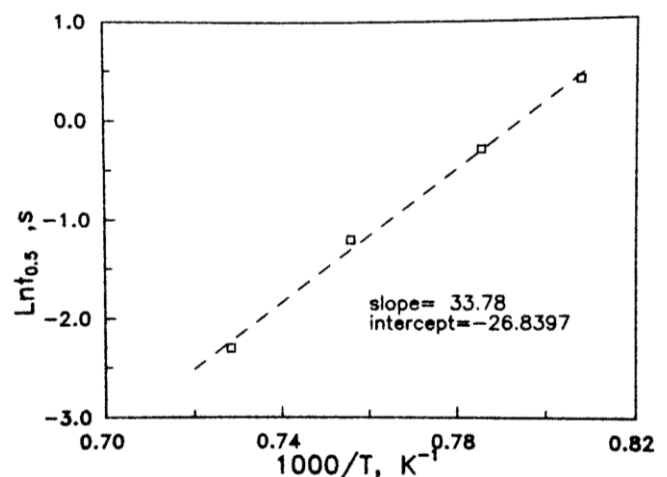


Figure.6. Time vs. Temperature Dependence at (965-1100°C).

IV. DISCUSSION

Activation energy for recrystallization is an energetic barrier that has to be overmatched for recrystallization to proceed. Mechanism of recrystallization includes two steps. Nucleation of recrystallized grains and growth of nuclei. Both processes are thermally activated, i.e. the reaction kinetics depends on the reaction temperature. In spite of the clear presence of these two processes, it is usually the overall value only is estimated, i.e. the activation energy for static recrystallization [1-11]. This simplification was necessary because modeling imposed a need for a constant that describes all softening processes (even sometimes including recovery).

Flow curves. The inter pass time has an effect on the shape of flow curves. In the case of longer interpass time as in figure 4a, there is no significant change in the shape of the second pass i.e. the flow curve of the second pass is characterized by a low yield strength and high strain hardening rate, implying that full recrystallization take place during delay time. On the other hand, in the case of short interpass time as in figure 4b, there is a significant change in both the shape of the second pass and the level of yield point, i.e. the flow curve of the second pass is characterized by a high yield strength and a low strain hardening rate, implying that recrystallization is fully/partially suppressed during delay time [1-6].

Fractional softening. To quantify the extent of softening during delay time, the fractional softening was calculated, using 0.1% offset method. Recrystallization is a process that consists of two steps: nucleation of strain free grains and growth of the nuclei etc. [7-9]. Also, the transformation is most intensive on new boundaries between deformed and recrystallized grains. Therefore, the process is auto-catalytically, which is in excellent agreement with the S shape of the curve [10]. Small increase of softened fraction at early stages is attributed to nucleation of strain free grains, while later acceleration of softening is attributed to growth of stable nuclei [8, 9]. At this moment, there is no general agreement how to correlate level of softening related to recovery separately from one related to recrystallization [10]. In this work, only total amount of softening will be discussed. The influence of temperature on recrystallization kinetics, table 3, is a direct consequence of the thermal activation nature of softening. Therefore, softening on lower temperature is expected to be shifted to longer times. Also, what is very important, the shape of all curves is similar, indicating that there is no change in reaction mechanism [8].

Avrami kinetics. Avrami exponent is very close to one, and shows very good agreement with previously published data [2, 3, 11-14]. This value indicates the nature of process, i.e. it is related to process that is characterized by nucleation on grain boundaries [2, 3, 7, 9-14]. A value of 281kJ/mol for activation energy is in very good agreement with previously published data [2,

3, 11-14]. This value is close to value of activation energy of diffusion of Nb in austenite [15]. Therefore, it is assumed that diffusion of Nb through grain boundary is the controlling step in recrystallization. In growth of stress free grains, the key factor is the mobility of grain boundaries. In temperature range tested in this work, Nb and other element were in solid solution, so that solution drag is the most important mechanism of controlling the mobility of grain boundaries. Activation energy obtained in this work is also in good agreement with values obtained using different testing methods (an isothermal testing and modeling), as shown in table 5. These values are valid in temperature range in which full recrystallization take place and all Nb is present in solid solution.

Table 5. Qsrx of Low Carbon Micro-Alloyed steel.

Method	Qsrx kJ/mol	Ref.
Isothermal tests	281	This work
Isothermal tests	258	16
Modeling	289	3

V. CONCLUSIONS

Low carbon micro-alloyed steel containing Nb and Ti was tested by means of two hit isothermal torsion with the aim to evaluate the interpass recrystallization data. Testing was performed in temperature range in which full recrystallization take place and all Nb is present in solid solution. The increase in test temperature decreases the time required for full recrystallization. Activation energy for static recrystallization estimated in this work on 281 kJ/mol is in the excellent agreement with previously reported both experimentally and modeled data. It indicates that the diffusion of Nb in austenite is most probably the rate controlling process i.e. presence of niobium in solution delays static recrystallization. The value of Avrami exponent $n_{SRX} = 1$, implies that the static recrystallization occurs at interface i.e. on grain boundaries, twins, deformation bands.

REFERENCES

- [1] F. Boratto et al, Thermec 88, ed. I. Tamura, ISIJ, Tokyo (1998), 383-391.
- [2] A. Laasraoui and J. J. Jonas, Metallurgical Transactions A, 22A (1991), 151-160.
- [3] S. F. Medina and A. Quispe, ISIJ International, 41 (2001), 774-781.
- [4] D.Q. Bai et al, Metallurgical Transactions A, 24A (1993), 2151-2159.
- [5] D. Drobnyak, A. Koprivica, N. Radovic, M. Andjelic, Steel Research, 68 (1997), 306-312.
- [6] N. Radovic, and D. Drobnyak, ISIJ International, 39 (1999), 575-582.
- [7] W. A. Johnson and R. F. Mehl, Transactions AIME, 135 (1939), 416.
- [8] D. Porter and K. Easterling, Phase Transformation in Metals and Alloys, Chapman and Hall, London (1992).
- [9] E. J. Palmiere, G. Garcia, A. J. DeArdo, Processing, Microstructure and Properties of Micro alloyed and other Modern High Strength Low Alloyed Steels, Ed. A.J. DeArdo, ISS, Warrendale, USA (1992), 113-133.
- [10] A. Fadel, IJEIT, Vol. 2, No. 2, (2016), 53-56.

- [11] P. D. Hodgson and R. K. Gibbs, *ISIJ International*, 32, (1992), 1329.
- [12] M. G Akben, J. J. Jones, Influence of multiple Micro alloy Additions On The Flow Stress And Recrystallization Behavior of HSLA Steels, *HSLA Steels Technology & Application*, Ed. Michael korchynsky, American Society For Metals, Pennsylvania, (1984), 149.
- [13] C.M. Sellars, The physical Metallurgy of Hot Working, In *Hot Working And Formation Processes* Ed. C. Msellars And G. J. Davies, The Metal Society, London (1980) 3.
- [14] C. M. Sellars and J. A. Whiteman, *Metal Science*, March-April, (1979), 187.
- [15] S. Kurokawa, J. E. Ruzzante, A. M. Hey and F. Dymant, *Metal Science* 17, (1983), 433-438.
- [16] F. S. Buffington, M. Hirano and M. Cohen, *Acta Merallurgica*, 9 (1961),434-469.
- [17] N. Radovic, D. Drobnjak, K. Raic, *Journal of Metallurgy*,15, (2009) 99.
- [18] N. Radovic, D. Drobnjak, Development of steels for fabrication of welded construction with improved safety, *Science- Research-Development*, 3, (2001), 81.
- [19] L. J. Cuddy, J. S. Lally, L. F. Porter, Improvement of Toughness in the HSLA of high heat input welds in ship steels. In *HSLA steels technology & application*, Ed. Michael Korchynsky, American Society For Metals, Pennsylvania (1984), 679.